



ELSEVIER

Contents lists available at ScienceDirect

Materials Letters

journal homepage: www.elsevier.com/locate/matlet

Competing anisotropic microstructures of $\text{Bi}_2(\text{Te}_{0.95}\text{Se}_{0.05})_3$ thermoelectric materials by Bridgman technique



Jintana Laopaiboon^a, Somkid Pencharee^a, Tossawat Seetawan^b, Ussadawut Patakham^c, Bralee Chayasombat^c, Chanchana Thanachayanont^{c,*}

^a Physics Department, Faculty of Science, Ubon Ratchathani University, 85 Sathollmark Rd. Warinchamrab, Ubon Ratchathani, Thailand, 34190

^b Thermoelectrics Research Center, Faculty of Science and Technology, Sakon Nakhon Rajabhat University, 680 Nittayo Rd., Sakon Nakhon, 47000 Thailand

^c National Metal and Materials Technology Center, 114 Thailand Science Park, Phaholyothin Rd., Klong 1, Klong Luang, Pathumthani 12120, Thailand

ARTICLE INFO

Article history:

Received 20 September 2014

Accepted 23 November 2014

Available online 2 December 2014

Keywords:

BiTeSe

Thermoelectric

Bridgman

Anisotropy

Orientation imaging microscopy

ABSTRACT

In this study, Bridgman technique was used to grow $\text{Bi}_2(\text{Te}_{0.95}\text{Se}_{0.05})_3$ thermoelectric materials. Pulling rates were varied at 0, 2, 4 and 8 mm/h. Anisotropic thermoelectric properties were investigated by measuring Seebeck coefficients, resistivities and power factors and microstructures by Orientation Imaging Microscopy (OIM) and X-ray diffraction, in the directions perpendicular and parallel to the pulling direction. An enhanced power factor of 2.01 mW/mK^2 in the direction parallel to the pulling direction was obtained for the pulling rate of 2 mm/h. The OIM result showed that infinitely long grains, with grain boundaries and crystal a-axis parallel to the pulling direction were responsible for the enhanced power factor. Competing effects of orientations of unit cells and grain boundaries were observed in all other samples.

© 2014 Elsevier B.V. All rights reserved.

1. Introduction

N-type $\text{Bi}_2(\text{Te}_{1-x}\text{Se}_x)_3$ solid solutions have been extensively investigated and coupled with p-type $(\text{Bi}_{1-y}\text{Sb}_y)_2\text{Te}_3$ in near room-temperature thermoelectric modules [1,2]. Whereas high figures of merit (ZTs) have been reported for nanostructured p-type $(\text{Bi}_{1-y}\text{Sb}_y)_2\text{Te}_3$ [3,4], matching n-type $\text{Bi}_2(\text{Te}_{1-x}\text{Se}_x)_3$ materials having high ZTs for high efficiency thermoelectric modules are still being sought for. The $\text{Bi}_2(\text{Te}_{1-x}\text{Se}_x)_3$ materials show good solid solubility at all compositions with uniaxial anisotropy in both electrical and thermal properties which are originated from the crystal structure [5,6]. The $\text{Bi}_2(\text{Te}_{1-x}\text{Se}_x)_3$ crystals are hexagonal having space group $R\bar{3}m$ with alternate $-\text{Te}(\text{Se})^{(1)}-\text{Bi}-\text{Te}^{(2)}-\text{Bi}-\text{Te}(\text{Se})^{(1)}-\text{Te}(\text{Se})^{(1)}$ - stacking sequence along the c-axis. The bonding of $\text{Te}(\text{Se})^{(1)}-\text{Te}(\text{Se})^{(1)}$ is a weak van der Waal's force resulting in cleavage planes being perpendicular to the c-axis.

In $\text{Bi}_2(\text{Te}_{1-x}\text{Se}_x)_3$ single crystals, both thermal and electrical conductivities in the direction parallel to the a-axis have been reported to be larger than that in the direction parallel to the c-axis. Although, the Seebeck coefficient showed only a slight difference in anisotropy, the overall figures of merit are strongly anisotropic [6]. Hu et al. [7] recently demonstrated that thermoelectric properties

of n-type bismuth telluride based alloys could be improved by microstructural modification through deformation-induced defects and texture enhancement. It was found that the n-type $\text{Bi}_2(\text{Te}_{1-x}\text{Se}_x)_3$ materials tended to be more (00 l) textured compared to the p-type $(\text{Bi}_{1-y}\text{Sb}_y)_2\text{Te}_3$.

In this study, Bridgman technique was used to grow $\text{Bi}_2(\text{Te}_{0.95}\text{Se}_{0.05})_3$ thermoelectric materials. Pulling rates were varied at 0, 2, 4 and 8 mm/h. Orientation Imaging Microscopy (OIM) was used to investigate microstructure and crystal structure of the n-type $\text{Bi}_2(\text{Te}_{0.95}\text{Se}_{0.05})_3$ thermoelectric materials.

2. Material and methods

Elemental powder mixtures of Bi (100 mesh, 99%), Te (200 mesh, 99.8%), Se (100 mesh, 99.5%) in compositional ratios of $\text{Bi}_2(\text{Te}_{0.95}\text{Se}_{0.05})_3$, were put into 75 ml stainless steel vials containing 5 mm and 10 mm stainless steel balls under an argon atmosphere. All chemicals were obtained from Sigma-Aldrich and used without further purification. The ratio of balls to material was 5:1 by weight. Mechanical alloying was applied using a planetary ball-milling machine, Fritsch model Pulverisette 7, operating at 500 rpm for 10 h. After milling the mechanically alloyed powders were put into a home-made Bridgman crystal grower. Ingots of $\text{Bi}_2(\text{Te}_{0.95}\text{Se}_{0.05})_3$ (150 mm in height, 20 mm in diameter, and 66.12 g in weight) were pulled at 0, 2, 4 and 8 mm/h., respectively.

* Corresponding author. Tel.: +66 564 6500; fax: +66 564 6447.

E-mail address: chanchm@mttc.or.th (C. Thanachayanont).

The crucible was made of graphite. The temperature was lowered gradually from 650 °C to 350 °C and a temperature gradient of about 25 °C/cm was obtained. The samples were then cooled down to room temperature at the rate of about 44 °C/h.

The ingots were cut into $4 \times 4 \times 10 \text{ mm}^3$ samples having the tall side parallel and perpendicular to the pulling direction, respectively. The crystal structure was investigated using XRD (Rigaku, TTRAX III) operated using $\text{CuK}\alpha$ radiation at 50 kV, 300 mA with a scanning speed of $5^\circ/\text{min}$ at 2θ steps of 0.02° . Then, the samples were polished using 800 μm SiC paper down to $1 \mu\text{m}$ diamond spray. The samples were then polished with a vibratory polisher using a $0.05 \mu\text{m}$ colloidal silica suspension. An optical Microscope (Carl Zeiss Model Axiolab A) was used to observe microstructure of the sample. A scanning electron microscope (SEM, Hitachi S-3400 N) operated at an accelerating voltage of 20 kV was used

together with OIM software TSL OIM Data collection 5.3. At each point, the Electron Backscatter Diffraction (EBSD) pattern is captured and automatically indexed to obtain the orientations of the grains and unit cells.

3. Results and discussion

The vertical Bridgman crystal growth system is one of the best techniques for the growth of semiconductor crystals. This technique provides steady temperature fields, controllable temperature gradients and purification [8]. The method yields large, pure crystals by controlling the heat and mass transfer boundary conditions. However, the melt/solid interface formed by Bridgman is a paraboloid with the center lower than the edges. It was shown that the

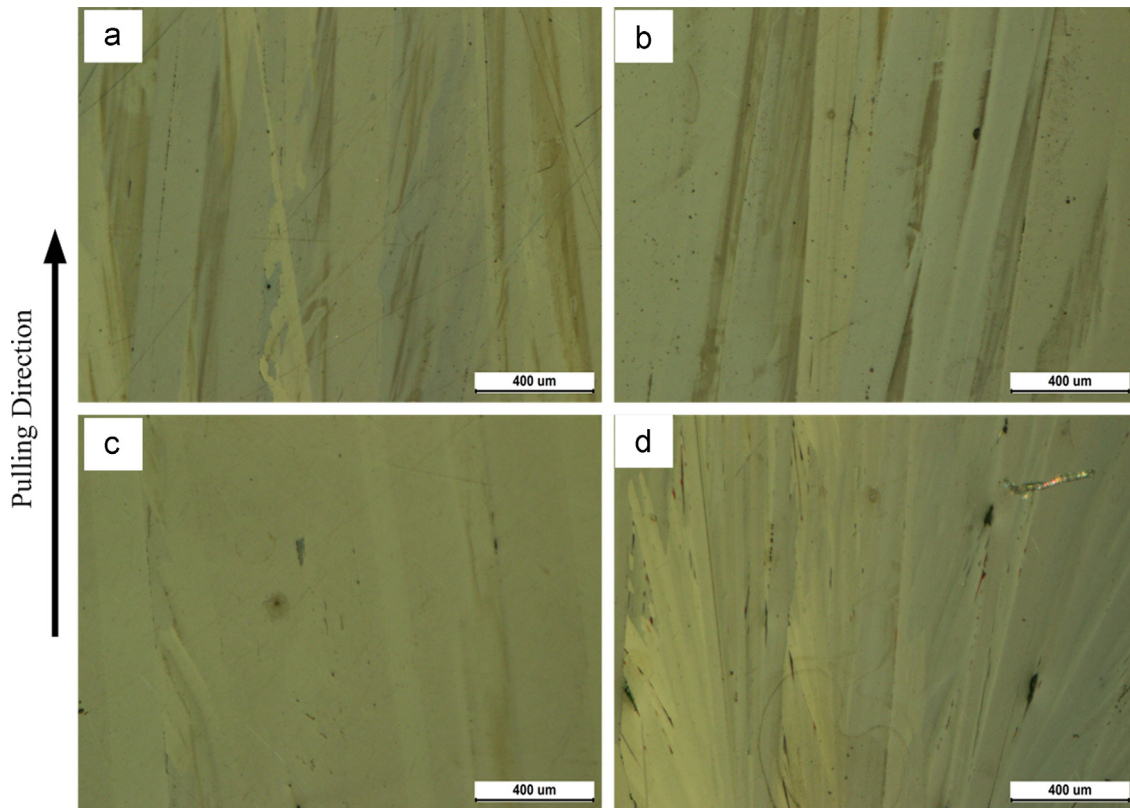


Fig. 1. Optical micrographs of Bridgman grown $\text{Bi}_2(\text{Te}_{0.95}\text{Se}_{0.05})_3$ ingots using pulling rates of (a) 0, (b) 2, (c) 4 and (d) 8 mm/h., respectively.

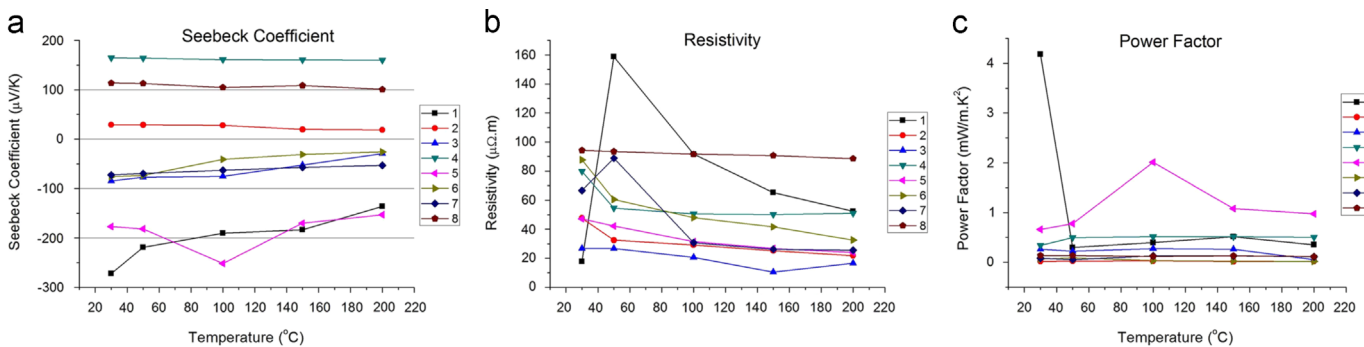


Fig. 2. (a) Seebeck coefficients (S), (b) resistivities (ρ) and (c) power factors ($=S^2/\rho$) of the Bridgman grown $\text{Bi}_2(\text{Te}_{0.95}\text{Se}_{0.05})_3$ ingots. 1–4 were pulled at 0, 2, 4 and 8 mm/h., respectively, and measured parallel to the pulling directions. 5–8 were pulled at 0, 2, 4 and 8 mm/h., respectively, and measured perpendicular to the pulling directions.

melt/solid interface is concave at the center and the solute concentration at the interface is not uniform. Increasing growth speed was found to result in more concave paraboloids. Figs. 1(a)–(d) show side-view optical micrographs of the $\text{Bi}_2(\text{Te}_{0.95}\text{Se}_{0.05})_3$ ingots grown using pulling rates of 0, 2, 4 and 8 mm/h., respectively.

The microstructures agree with the Bridgman growth geometry and physical domains in the melt [8]. Figs. 2(a)–(c), respectively, show Seebeck coefficients (S), resistivities (ρ) and power factors ($=S^2/\rho$) of the Bridgman grown $\text{Bi}_2(\text{Te}_{0.95}\text{Se}_{0.05})_3$ ingots using pulling rates of 0, 2, 4 and 8 mm/h., measured in perpendicular and parallel directions to the pulling direction. An enhanced power factor of 2.01 mW/mK² measured in the direction parallel to the pulling direction was obtained for the $\text{Bi}_2(\text{Te}_{0.95}\text{Se}_{0.05})_3$ crystal pulled at 2 mm/h.

Fig. 3 shows XRD patterns taken from the crystal pulled at 2 mm/h in the direction parallel and perpendicular to the pulling direction. The lattice constants determined from the XRD peaks are $a=4.41$ Å and $c=30.52$ Å. The XRD results suggested (0 1 20) be the preferred orientation in the parallel direction to the pulling direction and (1 1 0) in the perpendicular direction to the pulling direction. The (0 1 20) is 2.8 degrees from (0 0 1). This indicated that the $\text{Bi}_2(\text{Te}_{0.95}\text{Se}_{0.05})_3$ unit cells aligned approximately perpendicular to the pulling direction. Fig. 4(a) and (b) show, respectively, SEM images and corresponding OIM images of the crystals pulled at 0, 2 and 8 mm/h in the direction parallel to the pulling direction. The results confirmed that the c -axes of the unit cells of the $\text{Bi}_2(\text{Te}_{0.95}\text{Se}_{0.05})_3$ crystal orient approximately perpendicular to the grain boundaries. For the pulling rate of 2 mm/h, the grain boundaries are approximately parallel to the pulling direction, hence the c -axes of the unit cells of the $\text{Bi}_2(\text{Te}_{0.95}\text{Se}_{0.05})_3$ crystal orient approximately perpendicular to the pulling direction.

In the sample with a controlled microstructure, that is, prepared using 2 mm/h. pulling rate, a higher Seebeck coefficient and a lower resistivity were obtained in the direction parallel to the pulling direction than in the direction perpendicular to the pulling direction. Single crystal solid solution $\text{Bi}_2(\text{Te}_x\text{Se}_{1-x})_3$ is well-known for its anisotropic nature. Due to such anisotropy, commercial Bi_2Te_3 -based ingots are generally fabricated by traditional unidirectional crystal-growth methods such as Bridgman, Czochralski and zone-melting techniques [7,9–11]. The solidified ingots have preferred crystalline orientation and show good thermoelectric performance along the plane perpendicular to the c -axis [6,7,9] and depending on the preparation technique [6,9].

N-type $\text{Bi}_2(\text{Te}_{0.95}\text{Se}_{0.05})_3$ thermoelectric materials with preferred orientation have also been fabricated through the spark plasma sintering (SPS) technique. The c -axis of the elongated elliptical grains in the sintered samples were preferentially orientated parallel to the pressing direction [9], that is, the grain boundaries were found to be perpendicular to the pressing direction. The anisotropy was investigated by measuring the electrical conductivities in the two directions perpendicular and parallel to the pressing direction. Maximum conductivities in a temperature range of 300–500 K were found to be around 2.0×10^5 and 1.0×10^5 S/m, measured in the direction perpendicular and parallel to the pressing direction, respectively. Their results indicated that a better conductivity was obtained in the direction parallel to the grain boundaries and perpendicular to the c -axis.

In agreement with previous work by Hu et al. [7] and Jiang et al. [9], the Bridgman n-type $\text{Bi}_2(\text{Te}_{0.95}\text{Se}_{0.05})_3$ ingot pulled at 2 mm/h. was found to consist of columnar infinitely long vertical grains having grain boundaries parallel to the pulling direction. OIM result (Fig. 4(b)) showed that crystal growth occurred parallel to the a -axis of the hexagonal unit cells along the low-index planes to minimize the surface energy when growing. Since the thermoelectric properties along the a -axis is superior to those along the c -axis, Bridgman technique with an appropriate pulling rate can result in grain boundaries being parallel to the a -axis of the crystal. The grain boundaries will, hence, have a minimum effect on electrical property along the a -axis direction, resulting in a maximized Seebeck coefficient, a minimized resistivity and a maximized power factor. Competing effects of unit cells and grain boundaries were observed in all other samples.

4. Conclusion

N-type $\text{Bi}_2(\text{Te}_{0.95}\text{Se}_{0.05})_3$ thermoelectric materials were grown using Bridgman technique. By varying pulling rates at 0, 2, 4 and 8 mm/h., an enhanced power factor of 2.01 mW/mK² measured in the direction parallel to the pulling direction was obtained for the $\text{Bi}_2(\text{Te}_{0.95}\text{Se}_{0.05})_3$ crystal pulled at 2 mm/h. The enhanced power factor was resulted from columnar infinitely long vertical grains having no grain boundaries perpendicular to the pulling direction. Moreover, the OIM result indicated that the a -axis of the $\text{Bi}_2(\text{Te}_{0.95}\text{Se}_{0.05})_3$ crystal orient parallel to the pulling direction, resulting in the enhanced power factor.

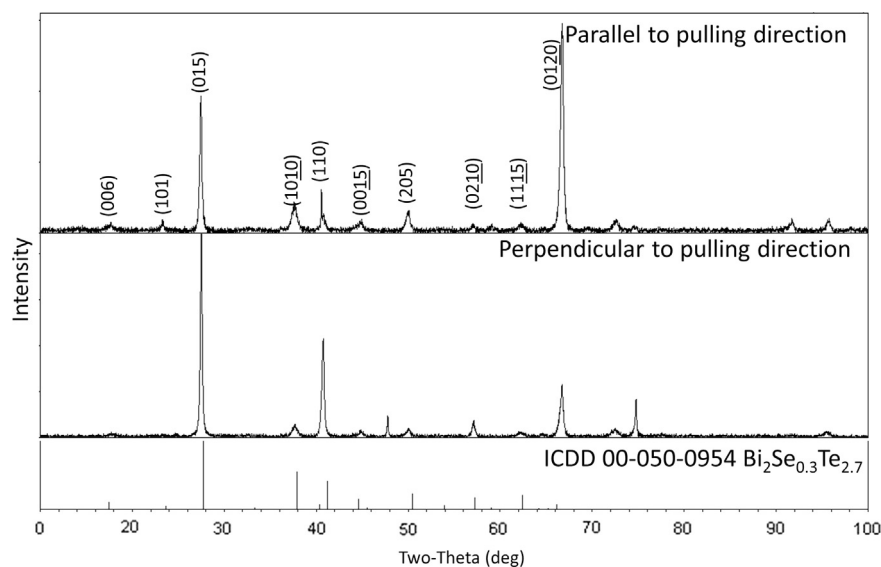


Fig. 3. X-ray diffraction (XRD) pattern of Bridgman grown $\text{Bi}_2(\text{Te}_{0.95}\text{Se}_{0.05})_3$ using pulling rate of 2 mm/h in parallel and perpendicular direction to the pulling direction.

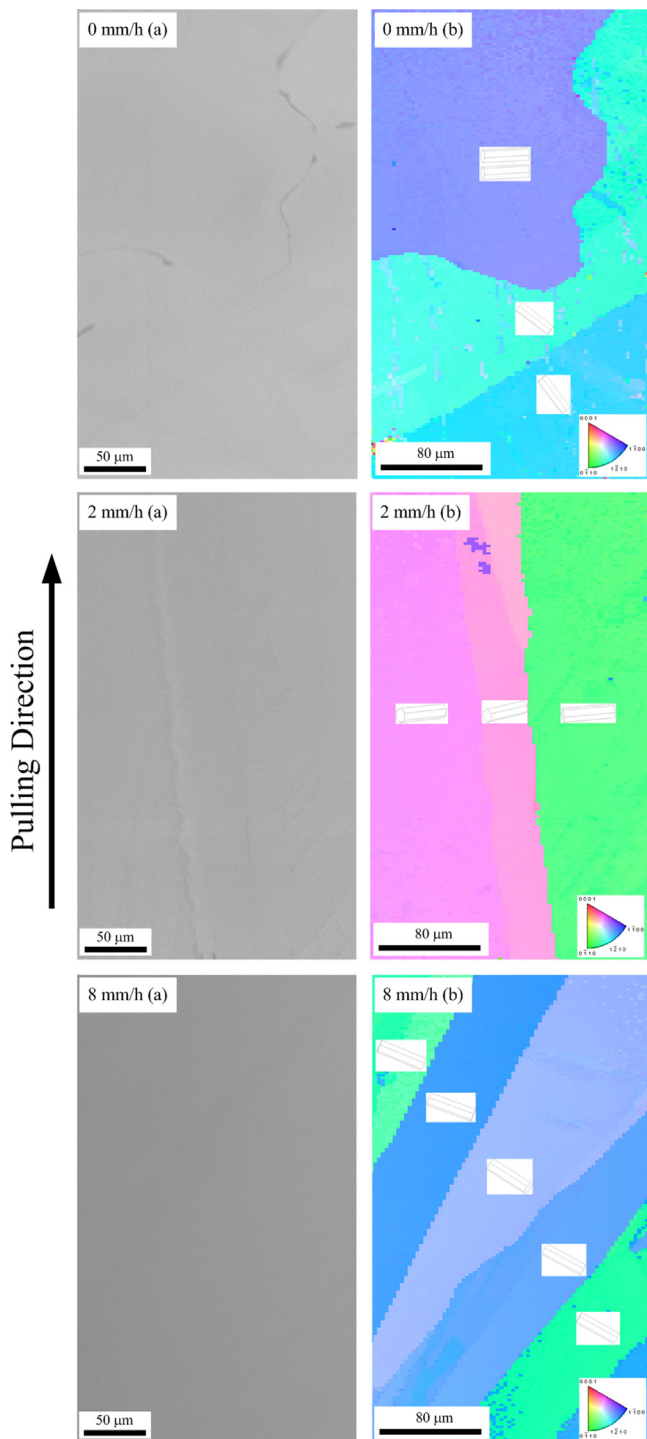


Fig. 4. (a) SEM micrographs and (b) corresponding OIM micrographs of Bridgman grown $\text{Bi}_2(\text{Te}_{0.95}\text{Se}_{0.05})_3$ using pulling rate of 0, 2 and 8 mm/h.

Acknowledgment

Authors would like to acknowledge the National Metal and Materials Technology Center for financial support (MTEC Grant No. MT-B-55-CER-07–295-I).

References

- [1] Majumdar A. Thermoelectricity in semiconductor nanostructures. *Science* 2004;303:777–8.
- [2] Suter C, Jovanovic ZR, Steinfeld A. A 1 kWe thermoelectric stack for geothermal power generation – modeling and geometrical optimization. *Appl Energy* 2012;99:379–85.
- [3] Venkatasubramanian R, Siivola E, Colpitts T, O'Quinn B. Thin-film thermoelectric devices with high room-temperature figures of merit. *Nature* 2001;413:597–602.
- [4] Poudel B, Hao Q, Ma Y, Lan Y, Minnich A, Yu B, et al. High-thermoelectric performance of nanostructured bismuth antimony telluride bulk alloys. *Science* 2008;320:634–8.
- [5] Wiese JR, Muldrew L. Lattice constants of Bi_2Te_3 - Bi_2Se_3 solid solution alloys. *J Phys Chem Solids* 1960;15:13–6.
- [6] Fukuda K, Imaizumi H, Ishii T, Toyoda F, Yamanashi M, Kibayashi Y. Orientation distribution and procedure parameters in hot pressed $(\text{Bi}_2\text{Te}_3)_{0.90}(\text{Bi}_2\text{Se}_3)_{0.10}$. International Conference on Thermoelectrics Conference Proceeding 1996:37–41.
- [7] Hu LP, Liu XH, Xie HH, Shen JJ, Zhu TJ, Zhao XB. Improving thermoelectric properties of n-type bismuth-telluride-based alloys by deformation-induced lattice defects and texture enhancement. *Acta Mater* 2012;60:4431–7.
- [8] Shi K, Liu J., Lu WQ. Numerical investigation of the interfacial characteristics during Bridgman growth of compound crystals. *Appl. Thermal Eng* 2007;27:1960–6.
- [9] Jiang J, Chen L, Bai S, Yao Q, Wang Q. Fabrication and thermoelectric performance of textured n-type $\text{Bi}_2(\text{Te},\text{Se})_3$ by spark plasma sintering. *Mat Sci Eng B* 2005;117:334–8.
- [10] Yamashita O, Tomiyoshi S, Makita K. Bismuth telluride compounds with high thermoelectric figures of merit. *J Appl Phys* 2003;93:368–74.
- [11] Zemskov VS, Belaya AD, Beluy US, Kozhemyakin GM. Growth and investigation of thermoelectric properties of Bi-Sb alloy single crystals. *J Cryst Growth* 2000;212:161–6.